

Recombinant botulinum neurotoxin serotype A1 in vivo characterization

Cindy Périer¹  | Vincent Martin¹ | Sylvie Cornet¹ | Christine Favre-Guilnard¹ | Marie-Noelle Rocher¹ | Julien Bindler² | Stéphanie Wagner² | Emile Andriambelison² | Brian Rudkin^{3,4} | Rudy Marty³ | Alban Vignaud¹ | Matthew Beard⁵  | Stephane Lezmi¹  | Mikhail Kalinichev¹ 

¹Ipsen Innovation, Les Ulis, France

²Neurofit SAS, Illkirch, France

³CARPACCIO.cloud, Lyon, France

⁴Univ Lyon, Université Lyon 1, INSERM, Stem Cell and Brain Research Institute U120, Bron, France

⁵Ipsen Bioinnovation, Abingdon, UK

Correspondence

Cindy Périer, Ipsen Innovation, 5, Avenue du Canada, 91940 Les Ulis, France.
Email: cindy.perier@ipsen.com

Funding information

Ipsen

Abstract

Clinically used botulinum neurotoxins (BoNTs) are natural products of *Clostridium botulinum*. A novel, recombinant BoNT type A1 (rBoNT/A1; IPN10260) has been synthesized using the native amino acid sequence expressed in *Escherichia coli* and has previously been characterized in vitro and ex vivo. Here, we aimed to characterize rBoNT/A1 in vivo and evaluate its effects on skeletal muscle. The properties of rBoNT/A1 following single, intramuscular administration were evaluated in the mouse and rat digit abduction score (DAS) assays and compared with those of natural BoNT/A1 (nBoNT/A1). rBoNT/A1-injected tibialis anterior was assessed in the in situ muscle force test in rats. rBoNT/A1-injected gastrocnemius lateralis (GL) muscle was assessed in the compound muscle action potential (CMAP) test in rats. The rBoNT/A1-injected GL muscle was evaluated for muscle weight, volume, myofiber composition and immunohistochemical detection of cleaved SNAP25 (c-SNAP25). Results showed that rBoNT/A1 and nBoNT/A1 were equipotent and had similar onset and duration of action in both mouse and rat DAS assays. rBoNT/A1 caused a dose-dependent inhibition of muscle force and a rapid long-lasting reduction in CMAP amplitude that lasted for at least 30 days. Dose-dependent reductions in GL weight and volume and increases in myofiber atrophy were accompanied by immunohistochemical detection of c-SNAP25. Overall, rBoNT/A1 and nBoNT/A1 exhibited similar properties following intramuscular administration. rBoNT/A1 inhibited motoneurons neurotransmitter release, which was robust, long-lasting, and accompanied by cleavage of SNAP25. rBoNT/A1 is a useful tool molecule for comparison with current natural and future modified recombinant neurotoxins products.

KEYWORDS

botulinum, muscle, neurotoxin, recombinant, rodent, SNAP25

Abbreviations: ANOVA, analysis of variance; BoNT, botulinum neurotoxin; CMAP, compound muscle action potential; c-SNAP25, cleaved SNAP25; D, day; DAS, digit abduction score; eSCN, embryonic spinal cord neuronal; GL, gastrocnemius lateralis; GPB, gelatin phosphate buffer; i.m, intramuscular; nBoNT/A1, natural BoNT type A1; NMJ, neuromuscular junction; rBoNT/A1, recombinant BoNT type A1; SEM, standard error of the mean; SNARE, sensitive factor attachment protein receptor; TA, tibialis anterior.

This is an open access article under the terms of the Creative Commons Attribution-NonCommercial-NoDerivs License, which permits use and distribution in any medium, provided the original work is properly cited, the use is non-commercial and no modifications or adaptations are made.

© 2021 The Authors. *Pharmacology Research & Perspectives* published by British Pharmacological Society and American Society for Pharmacology and Experimental Therapeutics and John Wiley & Sons Ltd.

1 | INTRODUCTION

Botulinum neurotoxins (BoNTs), produced by *Clostridium botulinum* and related bacteria, are the most potent toxins known. The BoNT serogroup comprises at least eight serotypes (A-G, X) and over 40 subtypes.²³ All BoNTs share the same three structural domains, the binding and translocation domains comprise a 100-kDa heavy chain and a catalytic domain comprises a 50-kDa light chain, these chains are linked by a disulfide bond.²⁹ Upon binding to cell surface receptors of nerve endings, BoNT is internalized and the catalytic domain is translocated into the cytosol where the disulfide bond is reduced. Once freed, the light chain cleaves specific soluble N-ethylmaleimide-sensitive factor attachment protein receptor (SNARE) proteins, inhibits fusion of synaptic vesicles with the presynaptic membrane, and blocks neurotransmitter release. Specifically, BoNT serotype A (BoNT/A) binds to synaptic vesicle protein isoforms 2A-C (SV2A-C) and cleaves Synaptosomal-Associated Protein of 25 kDa (SNAP25) on the plasma membrane of presynaptic terminal of neurons.²⁴ It inhibits acetylcholine (ACh) release at the neuromuscular junction (NMJ) which leads to the characteristic flaccid paralysis observed in botulism.²⁹

A growing number of medical and esthetic applications use A1 and B1 BoNT subtypes purified from *Clostridium botulinum*. Currently, several commercial formulations of BoNT/A1 (Botox[®], Dysport[®], Xeomin[®]) are approved for cosmetic uses as well as for therapeutic indications such as upper and lower limb spasticity in adults and children, dystonia, blepharospasm, hypersalivation, overactive bladder, and migraine.³² While the commercially available neurotoxins are sourced from native *Clostridium botulinum* bacterial hosts, there are growing efforts to develop recombinant neurotoxins using other expression hosts such as *Escherichia coli*. For example, recombinant BoNT serotypes A, B, C, D, E, and F have been well-characterized in vitro and in vivo.³⁷ In addition, recombinant BoNT/E has been tested in a clinical trial and has shown efficacy in reducing the compound muscle action potential (CMAP) in the extensor digitorum brevis of healthy volunteers.²⁵

A novel, recombinant BoNT/A1 (rBoNT/A1) has been synthesized using the native amino acid sequence expressed in *E. coli* using already established methods.^{14,36} It has been characterized in vitro and ex vivo and confirmed to be biochemically and functionally comparable with native BoNT/A1 (nBoNT/A1)¹⁵. Specifically, rBoNT/A1 was as efficacious as nBoNT/A1 in inhibiting ACh release by cleaving SNAP25, as demonstrated in a cell-based assay of rat embryonic spinal cord neurons and in ex vivo mouse phrenic nerve hemidiaphragm assay.

The aim of the current study was to characterize the properties of rBoNT/A1 in vivo. First, we aimed to compare the properties of rBoNT/A1 with those of nBoNT/A1 in an assay reflecting the functional activity of a skeletal muscle, the digit abduction score (DAS) assay, in mice and rats. The DAS assay is based on the reflexive spread of digits in rodents and is used to measure local paralysis after intramuscular (i.m.) injection of BoNT into the hindleg.^{1,2,5} The dose-effect relationship between the amount of injected BoNT and

its local paralytic effect allows for the determination of BoNT potency, onset, and duration of action. Second, we aimed to further characterize the functional activity of rBoNT/A1 by evaluating its effects on the contractile and electrical properties of injected muscle and its morphology using the in situ muscle force assay. This assay measures the force generated by the injected muscle after electrical sciatic nerve stimulation.²⁰ Third, we aimed to measure compound muscle action potential (CMAP) to evaluate the effect of BoNT on the electrical properties of the muscle over a 30-day period. Change in CMAP amplitude is a sensitive measure of BoNT activity in terms of onset, time to peak, and duration.^{31,33} Furthermore, we aimed to assess the effect of rBoNT/A1 on muscle morphology by measuring muscle weight, volume, and fiber size, as nBoNT/A1-based products are known to induce muscle atrophy in preclinical models^{18,34,35} and in the clinic.¹¹ Finally, we aimed to confirm the enzymatic activity of rBoNT/A1 in injected muscle via immunohistochemical detection of cleaved SNAP25 (c-SNAP25).

2 | MATERIALS AND METHODS

2.1 | Animals

Adult male CD-1 mice were purchased from Charles River Laboratories and housed six per cage. Adult, female Sprague-Dawley rats were purchased from Janvier Labs, housed two to four per cage and remained in free estrous cycle when tested. We used female rats as they are slower to gain body weight compared with males and easier to handle in experiments involving longitudinal testing. Mice and rats housed in the Ipsen Innovation animal facility were kept on a 12 h light/dark cycle (lights on from 07:00 to 19:00). Rats housed in the Neurofit animal facilities were kept on a reversed 12 h light/dark cycle (lights on from 18:00 to 06:00). All animals were maintained in an enriched environment under a constant temperature ($22 \pm 2^\circ\text{C}$) and humidity ($55\% \pm 5\%$) with food and water available ad libitum. Animals were acclimatized for at least 7 days prior to experimentation.

Experimental procedures were reviewed and approved by the Ethics Committees of Ipsen Innovation (C2EA) and Neurofit (CEEA). Studies were performed in full compliance with the ARRIVE guidelines, European Communities Council Directive 2010/63/EU and French National Committee decree 87/848.

All in vivo experiments were performed within Ipsen laboratories, except for the CMAP assay, which was performed at Neurofit.

2.2 | BoNT

rBoNT/A1 gene synthesis, expression in *E. coli*, and purification methods are described by Hooker et al.¹⁵ rBoNT/A1 activity in vitro was confirmed through cell-based assays (SNAP25 cleavage) using rat embryonic spinal cord neuronal (eSCN) cultures. rBoNT/A1 activity ex vivo was shown in the mouse phrenic nerve hemidiaphragm.¹⁵

Research-grade purified nBoNT/A1 (150 kDa) was purchased from List Biological Laboratories. The molecular activity was previously confirmed in glycine and glutamate release assays, in SNAP25 cleavage using either rat eSCN or spinal cord neuronal cultures, and in the mouse nerve phrenic hemidiaphragm assay.^{10,15} nBoNT/A1 was reconstituted in 1 mg/ml bovine serum albumin (Sigma-Aldrich) in Dulbecco's phosphate-buffered saline (Sigma) to obtain a 0.1 mg/ml stock solution that was stored at -80°C as single-use aliquots. rBoNT/A1 was stored at -80°C , as single-use aliquots, at 0.1 mg/ml in phosphate-buffered saline (KH_2PO_4 1 mM, Na_2HPO_4 3 mM, NaCl 155 mM, pH 7.4). Working solutions were prepared with gelatin phosphate buffer (GPB) to yield the final desired concentrations (see below). GPB was prepared using 0.2% v/v gelatin (Prionex®, Sigma), 0.7% w/v Na_2HPO_4 (Emsure®, Merck), and sterile water for irrigation (Ecotainer®, Aqua B. Braun). The final pH was adjusted to 6.5 using orthophosphoric acid (85%; Merck).

2.3 | DAS assay in mice

The mouse DAS assay was performed as described previously.² Mice were suspended briefly by the tail to elicit a typical startle response characterized by hindlimb extension and abduction of digits. The digit abduction response of each mouse was scored live using a 5-point scale, from normal reflex/no inhibition (DAS 0) to full inhibition of digit abduction (DAS 4). Male CD-1 mice (24–30 g) were prescreened for a normal digit abduction response before the experiment; those showing abnormal digit abduction responses or hind paw deformities were excluded. Animals were randomized before the experiment to obtain comparable mean body weight in each group.

Mice were anaesthetized with a 3% isoflurane/oxygen mixture prior to BoNT/A1 or vehicle administration. Using a 30-gauge needle attached to a 100 μl syringe (SGE Analytical Science, Interchim), the needle was inserted into the gastrocnemius–soleus muscle complex of the right hindlimb and a fixed 20 μl volume was injected. Both nBoNT/A1 and rBoNT/A1 molecules were evaluated in independent experiments (each performed in duplicate). rBoNT/A1 was injected at 0.26, 0.40, 0.59, 0.89, 1.33, 2.00, 3.00, 4.40, 6.70, 10, and 15 pg/mouse, whereas nBoNT/A1 was injected at 0.89, 1.33, 2.00, 3.00, 4.40, 6.70, 10, and 15 pg/mouse ($n = 6/\text{dose}/\text{experiment}$). A control group ($n = 6$) injected with vehicle (GPB) was included in each experiment. All DAS scoring was performed blinded by the same operator and was conducted 8 h post administration, then once a day for 4 consecutive days. The body weight assessment and monitoring of clinical signs was performed daily. At the experiment end, or earlier if considered necessary, animals were euthanized by CO_2 asphyxiation.

2.4 | DAS assay in rats

The rat DAS assay was performed as described previously.⁵ The hindlimb digit abduction reflex was induced by grasping the animal lightly around the torso and lifting it swiftly into the air or by lifting

it with the nose pointing downward. The digit abduction response of each rat was scored on a 5-point scale, from normal reflex (DAS 0) to full inhibition of the digit abduction reflex (DAS 4). Female Sprague-Dawley rats (170–200 g, $n = 6/\text{dose}/\text{experiment}$) were prescreened for a normal digit abduction response; those showing abnormal digit abduction responses or hind paw deformities were excluded from the study. Animals were randomized before the experiment to obtain comparable mean body weight in each group.

Under 3% isoflurane/oxygen anesthesia, rats were administered with 10 μl of BoNT/A1 or vehicle into the peroneal muscle complex using an identical dose range (0.50, 1.00, 2.50, 5.00, and 10 pg/rat) for each toxin, with a control group ($n = 6$) injected with vehicle (GPB) included in each experiment. DAS scoring was performed 7 h post-administration, twice a day on days D1–D3 for nBoNT/A1, once on D4, and once per day on D6 and D7 or D5 and D7 for nBoNT/A1 and rBoNT/A1, respectively. Experiments (each tested in duplicate independent experiments) were blinded, with scoring performed by the same operator, and body weight recorded daily. At the experiment end, or earlier if considered necessary, animals were euthanized by CO_2 asphyxiation.

2.5 | In situ muscle force test

The in situ muscle force test was adapted from the method described by Ma et al.²⁰ to record muscle force from the tibialis anterior muscle. Female rats (210–270 g) were anaesthetized with 3% isoflurane/oxygen before receiving a single injection (250 $\mu\text{l}/\text{kg}$ body weight) of rBoNT/A1 (0.30, 1.00, 3.00, and 10 pg/kg) or vehicle (GPB, $n = 6/\text{group}$), through the skin, into the belly of the left tibialis anterior muscle. Based on our findings from the rodent DAS assays, muscle force measurements were performed 3 days post-administration. After rBoNT/A1 injection, animals received a subcutaneous injection of buprenorphine (0.01 mg/kg), followed by intraperitoneal injection of a ketamine (40 mg/kg) and xylazine (15 mg/kg) mix 30 min later. Animals were weighed daily from the day of injection (D0) to D3. On D3, animals were anaesthetized with 3% isoflurane/oxygen. The tibialis anterior muscle was then exposed, and its distal tendon was cut and attached to a force transducer (Aurora Scientific Europe) with a silk suture. The sciatic nerve was exposed at the level of the hip and the knee and foot were fixed with clamps. Isometric contraction of the tibialis anterior was induced by stimulating the sciatic nerve with a bipolar electrode at 100 Hz, 10 mA, 300 ms (610A Dynamic Muscle Control LabBook software, Aurora Scientific). The absolute maximal force was determined at optimal length (length at which maximal tension was obtained during tetanus) and expressed in Newtons (N, 611A Dynamic Muscle Analysis software, Aurora Scientific). At the experiment end, the rats were euthanized by intraperitoneal sodium pentobarbital injection; the injected/ipsilateral and non-injected/contralateral tibialis anterior were then collected for muscle weight assessment. The calculated muscle force was normalized to muscle mass (also called the estimate of specific maximal force sP0) and expressed as N/g of muscle.

2.6 | CMAP

CMAP assessment was performed as previously described⁶ and recording was performed with a Keypoint electromyograph (Medtronic). Subcutaneous monopolar needle electrodes (No 9013R0312; Medtronic) were used for both stimulation and recording. A ground electrode was placed in the paw pad of the recorded hind paw. The sciatic nerve was stimulated with a single pulse (12.8 mA of 0.2 ms duration) by a monopolar needle placed at the sciatic notch. CMAP was recorded by needle electrodes placed into the center of the gastrocnemius lateralis muscle. Female rats were anaesthetized using a 2–3% isoflurane/oxygen mixture and placed in a prone position. Once the electrodes were implanted, stimulation of the sciatic nerve and CMAP recording in the gastrocnemius muscle were performed. After recording, the animal was returned to its home cage.

We chose to explore rBoNT/A1 onset and duration of action at the 0.5 pg/kg dose, which we observed to trigger a submaximal reduction in CMAP amplitude in the injected muscle. A week prior to D0, a baseline CMAP measurement was performed on two groups of rats (170–190 g, $n = 8$ –12/group). Animals were randomized to obtain comparable mean body weight in each group. Animals received a 20 μ l i.m. injection of rBoNT/A1 (0.50 pg/kg) or vehicle (GPB) into the right gastrocnemius lateralis. CMAP amplitudes were measured in the same muscle on post-injection D1, D2, D3, D6, D10, D20, and D30 after which animals were euthanized by CO₂ asphyxiation.

2.7 | Muscle atrophy and immunohistochemical analysis of c-SNAP25

Female rats (170–200 g, $n = 6$ /group) were anesthetized with an isoflurane/oxygen mixture before receiving a 20 μ l i.m. injection of vehicle (GPB) or rBoNT/A1 (1.00, 5.00, 25, 50, 100, and 200 pg/kg) into the right gastrocnemius lateralis. We chose a range of doses based on early findings that they did not cause changes in body weight gain. Thirty days after administration (corresponding to the time of previously observed maximum BoNT/A1-induced myofiber atrophy in rats), animals were deeply anesthetized with 5% isoflurane and euthanized via exsanguination before both right (ipsilateral, injected) and left (contralateral, noninjected) gastrocnemius lateralis muscles were harvested. Muscles were weighed and their volume measured using a plethysmometer (Bioseb).

Harvested muscles were fixed in 10% v/v formalin (VWR Chemicals) for 48 h and following a dehydration protocol, muscles were embedded in paraffin blocks and histologic slides were prepared. A cross-section taken at the level of the muscle belly was used to calculate muscle fiber area, and an adjacent section was used for immunohistochemical detection of SNAP-25 cleaved by rBoNT/A1 (c-SNAP25).

To determine muscle fiber area, tissue sections were stained with a reticulin contrast kit (Biognost), allowing identification and

segmentation of myofibers. Stained slides were scanned and key parameters for each fiber were automatically derived from images of individual cross-sections using the CARPACCIO.cloud algorithms adapted for reticulin staining,³⁰(<http://www.carpaccio.cloud>). Fiber area frequency distribution was calculated by determining the number of fibers within intervals of $0.1 \times 10^3 \mu\text{m}^2$ and dividing by the total number of fibers in the cross-section.

For immunohistochemical c-SNAP25 staining, an in-house primary rabbit polyclonal antibody (EF14007, Ipsen Innovation) specific to BoNT/A1 cleaved form of SNAP25 was used. This antibody specificity was tested by assessing staining colocalization with a mouse monoclonal antibody for the SNAP25 N-terminal part (SYSY 111 011, Synaptic Systems) in rats injected muscle treated with vehicle or rBoNT/A1 highest dose of 200 pg/kg. After a heat-induced epitope retrieval step, endogenous peroxidases were blocked for 10 min in a 3% H₂O₂ solution. The sections were incubated with the two primary antibodies EF14007 and SYSY 111 011. Sections were then incubated with the appropriate secondary antibodies (Alexa555-conjugated and Alexa488-conjugated for EF14007 and SYSY 111 011 respectively, Thermo Scientific). Finally, slides were mounted using DAPI Fluoromount G (Thermo Scientific). Images were collected using an Olympus Microscope BX43F equipped with epifluorescence and processed using GIMP software. For quantification of c-SNAP25 staining in rat muscles, a standard avidin-biotin-peroxidase procedure was used. After heat-induced epitope retrieval and endogenous peroxidases blocking steps, sections were incubated with EF14007. They were then incubated with a biotinylated anti-rabbit immunoglobulin G, secondary antibody for 30 min (Vector Laboratories), followed by a 30-min incubation with an amplification system (avidin-biotin) coupled with horseradish peroxidase (Vector Laboratories). Finally, sections were incubated for 5 min with a 0.02% diaminobenzidine solution (DAKO), counterstaining was performed using hematoxylin, and the slides were visualized under the light microscope. The amount of c-SNAP25 in the tissues was determined by a 5-point scale scoring system, based on a combination of criteria, that is, intensity and density of NMJ staining and the presence of staining in terminal nerve endings and larger intramuscular nerves (Table 1).

2.8 | Data and statistical analysis

The data and statistical analysis of this study fully comply with the recommendations on experimental design and analysis in pharmacology.^{8,9} All data in the text and figures are presented as mean \pm standard error of the mean (SEM) and statistical significance was set to $p < 0.05$.

For the mice and rat DAS assay, the highest average DAS score (mean DAS max) per dose group was plotted against the natural logarithm of each dose. A four-parameter logistic equation curve was fitted, with the lower and upper asymptotes constrained to 0 and 4, respectively. The dose resulting in half-maximal DAS value (DAS 2, ED₅₀) was calculated from the equation. The DAS 4 dose was defined

Score	Criteria
1	Very few and/or very weak/partial staining of NMJ only
2	Some moderate staining of frequent NMJ No staining of terminal nerve endings No staining of intramuscular nerves (± 10 axons in thickness)
3	Strong staining of numerous NMJ Strong staining of terminal nerve endings No staining of intramuscular nerves (± 10 axons in thickness)
4	Strong staining of numerous NMJ Strong staining of terminal nerve endings Strong staining of intramuscular nerves (± 10 axons in thickness)

TABLE 1 Scoring system used for the quantification of c-SNAP25 in muscles using immunohistochemical labeling

as the first experimental dose inducing the mean DAS value of 4 for that dose group. The ED_{50} of nBoNT/A1 and rBoNT/A1 were compared using Student's *t* test for statistical significance. Body weight data were analyzed using a one-way analysis of variance (ANOVA) and post-hoc Dunnett's test for multiple comparisons.

In situ muscle force values were normalized, plotted against the doses and fitted with a Weibull growth curve adjusted with the following equation: %inhibition = $a \cdot (1 - \exp(-(dose/b)^c))$, where *a* is the high asymptote, *b* is the inflection point, and *c* is the growth rate. The dose that induced inhibition of 50% of the maximal normalized force (ED_{50}) was calculated from the control group. For ipsilateral and contralateral sides, sPO and muscle weight were analyzed using a one-way ANOVA followed by an adjusted Student's *t* test for significance with respect to the vehicle-treated group. Body weights were analyzed using a two-way repeated measure analysis of covariance followed by Dunnett's post hoc test.

For muscle weight and volume analysis, mean values from BoNT/A1 and vehicle-injected rats were compared using a two-way ANOVA followed by Tukey's multiple comparison test.

For c-SNAP25 staining analysis, the mean of each group from BoNT/A1-injected rats was compared with vehicle-injected rats using a Kruskal-Wallis test followed by uncorrected Dunn's test.

Muscle fiber area frequency distribution was analyzed from data automatically derived from images of individual muscle cross-sections. Results from each cohort were calculated by taking the mean \pm SEM at each interval and the significance of the linear association between doses was calculated using the Pearson correlation coefficient.

3 | RESULTS

3.1 | DAS assay in mice

Following i.m. administration of rBoNT/A1 and nBoNT/A1 at 0.89–10 pg/mouse, mean [95% CI range] ED_{50} values for rBoNT/A1 and nBoNT/A1 were 1.3 [1.17–1.56] and 1.6 [1.32–1.96] pg/mouse, respectively (Figure 1A). For both BoNT/A1 molecules, rapid and dose-dependent increases in DAS were observed (Figure 1B). Mice treated with either BoNT/A1 showed maximal inhibition of the digit abduction (DAS 4) 1–2 days after treatment. The doses causing the half-maximal (1.33 pg/mouse) and maximal inhibition (10 pg/mouse)

of digit abduction were similar for both BoNT/A1 molecules, as were their time course profiles (Figure 1B).

Both rBoNT/A1 and nBoNT/A1 injections affected body weight gain. Specifically, animals treated between 1.33 and 4.40 pg/mouse of rBoNT/A1 gained less weight than vehicle-treated controls. Animals treated at 6.70 pg/mouse rBoNT/A1 gained no weight, whereas those treated at 10 pg/mouse lost body weight (Figure 1C). Similarly, animals treated between 3.00 and 4.40 pg/mouse of nBoNT/A1 gained less body weight than vehicle-treated controls, whereas those treated at 6.70 and 10.00 pg/mouse lost body weight (Figure 1C). Changes in body weight gain following treatment of either BoNT/A1 were most pronounced between 3 and 4 days post-injection (Figure 1C). In one experiment per compound, animals treated at 15 pg/mouse showed clinical signs (ruffed fur, abdominal ptosis, palpebral ptosis) associated with a BW loss above 20%. These animals were humanely euthanized before the experiment end, the data were excluded from the analysis and the dose was excluded from further studies.

3.2 | DAS assay in rats

Following i.m. administration of rBoNT/A1 and nBoNT/A1 at 0.50–10 pg/rat, mean [95% CI range] ED_{50} values for rBoNT/A1 and nBoNT/A1 were 0.8 [0.60–1.08] and 1.3 [1.05–1.58] pg/rat, respectively (Figure 2A). Both BoNT/A1 molecules caused rapid and dose-dependent increases in DAS (Figure 2B). rBoNT/A1 and nBoNT/A1-treated animals showed maximal inhibition of digit abduction (DAS 4) 1–2 days after dosing. The doses causing the half-maximal (1.00 pg/rat) and maximal inhibition (10 pg/rat) of digit abduction were similar for both BoNT/A1 molecules (Figure 2B).

At the dose range tested, neither rBoNT/A1 or nBoNT/A1 had any effect on body weight gain up to 7 days of testing (Figure 2C).

3.3 | In situ muscle force test

A single i.m. administration of rBoNT/A1 dose dependently decreased the muscle force generated by nerve stimulation of the ipsilateral tibialis anterior. Specifically, 0.30, 1.00, 3.00, and 10 pg/kg rBoNT/A1 caused 17%, 50%, 74%, and 92% reductions in muscle force compared with that of vehicle-treated animals (all $p < 0.05$;

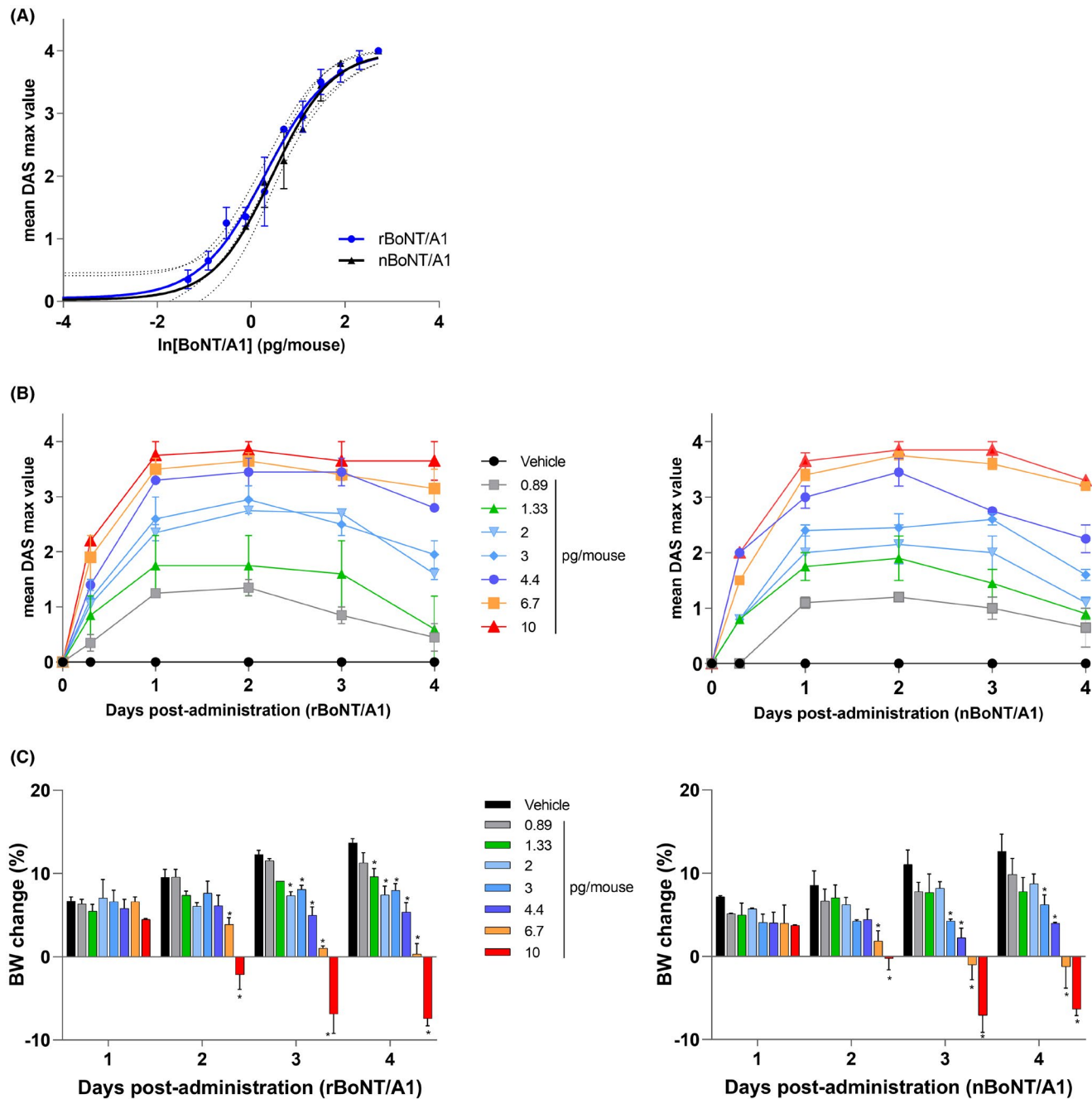


FIGURE 1 (A) Mean peak digit abduction score (DAS) curves of rBoNT/A1 or nBoNT/A1 (0.89–10 pg/mouse) 2–3 days post-administration into the gastrocnemius–soleus muscle complex of male CD-1 mice. (B) Time course of DAS following i.m. injection of rBoNT/A1 (left panel) and nBoNT/A1 (right panel) or corresponding vehicle (GPB). (C) Percentage change in body weight (vs. Day 0) after i.m. administration of rBoNT/A1 (left panel) or nBoNT/A1 (right panel) in the same experiments. Doses closest to the ED_{50} and DAS 4 values are in green and red, respectively. All values are mean \pm SEM from two independent experiments ($n = 6/\text{dose}/\text{experiment}$). * $p < 0.05$ compared with the vehicle-treated group (black)

Figure 3A). The ED_{50} of rBoNT/A1 was estimated at 1.20 pg/kg [0.67–1.64]. Overall, rBoNT/A1-injected tibialis anterior showed a tendency to weigh less than those injected with vehicle. The difference in weight between rBoNT/A1-injected and vehicle-injected tibialis anterior was greatest and statistically significant (12%; $p < 0.05$) at the highest dose (10.00 pg/kg; Figure 3B). The weight of the contralateral tibialis anterior was not affected by treatment (Figure 3C).

3.4 | CMAP

An acute i.m. administration of 0.50 pg/kg rBoNT/A1 into the rat gastrocnemius lateralis resulted in a rapid decrease of CMAP amplitude, with a reduction of 56.5% on D1 and 70.3% on D6 (Figure 4A). Thereafter, CMAP amplitude showed gradual recovery. By D30, inhibition of CMAP amplitude was reduced to

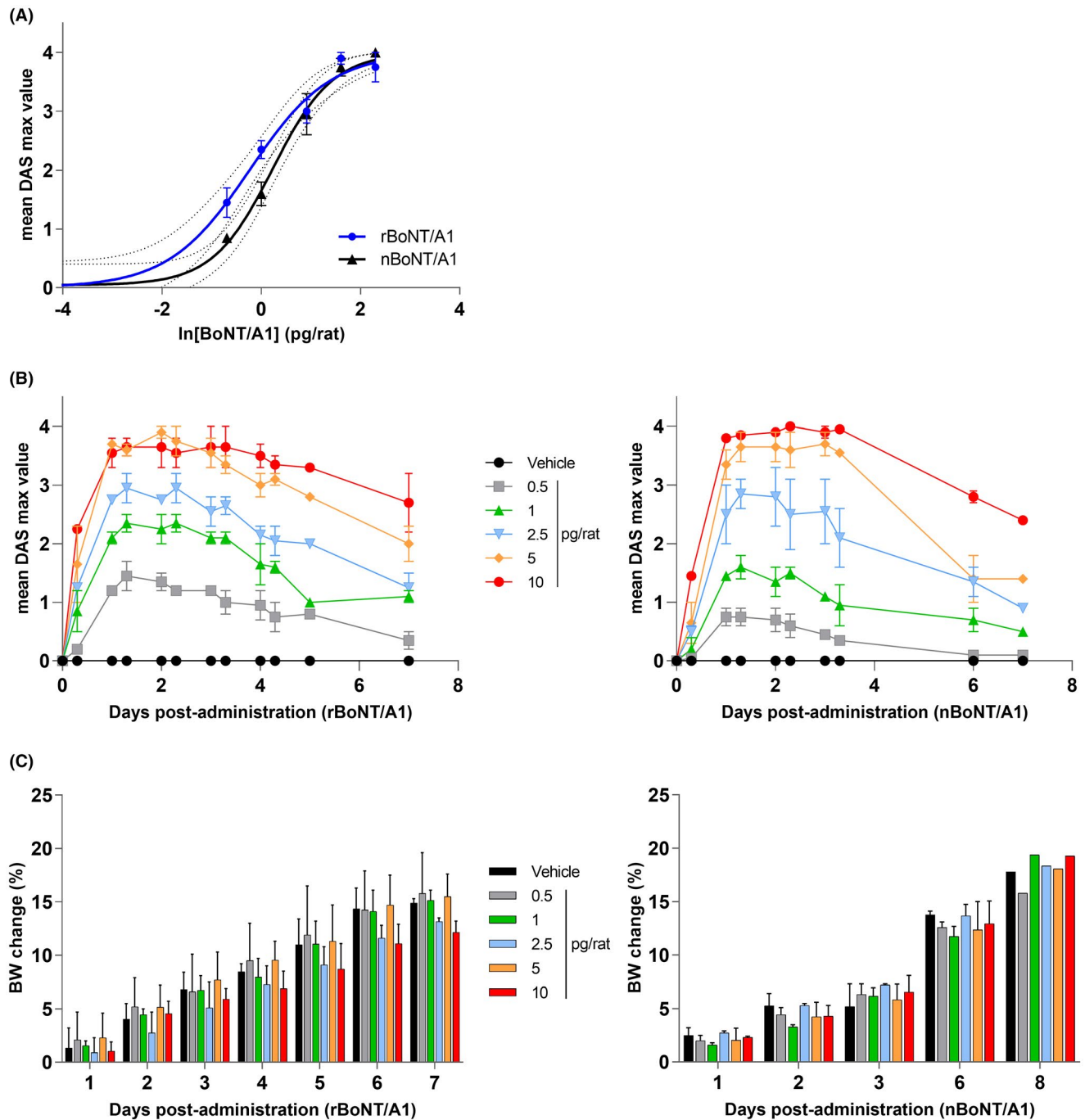


FIGURE 2 (A) rBoNT/A1 and nBoNT/A1 dose–response (0.5–10 pg/rat) in the digit abduction score (DAS) assay following a single i.m. injection into the peroneal muscle complex in rats. The curves correspond to mean peak DAS responses observed 2–3 days post-administration. (B) Time course of DAS following i.m. injection of either rBoNT/A1 or nBoNT/A1 (0.5–10 pg/rat) or vehicle (GPB) into the peroneal muscle in rats. (C) Percentage change in body weight (vs. day 0) after i.m. administration of rBoNT/A1 (left panel) and nBoNT/A1 (right panel) in the same experiments. Doses closest to the ED₅₀ and DAS 4 values are in green and red, respectively. All values are mean \pm SEM from two independent experiments ($n = 6$ /dose/experiment)

30%. rBoNT/A1 (0.50 pg/kg) had no effect on CMAP amplitude of the contralateral gastrocnemius lateralis. The representative CMAP recordings at baseline (Day 7) and 24 h (Day 1) after vehicle or rBoNT/A1 0.5 pg/kg administration are presented in Figure 4B.

3.5 | Muscle atrophy

A single i.m. injection of rBoNT/A1 (1.00–200 pg/kg) into the gastrocnemius lateralis resulted in a dose-dependent decrease in muscle weight when assessed 30 days post-injection (Figure 5A).

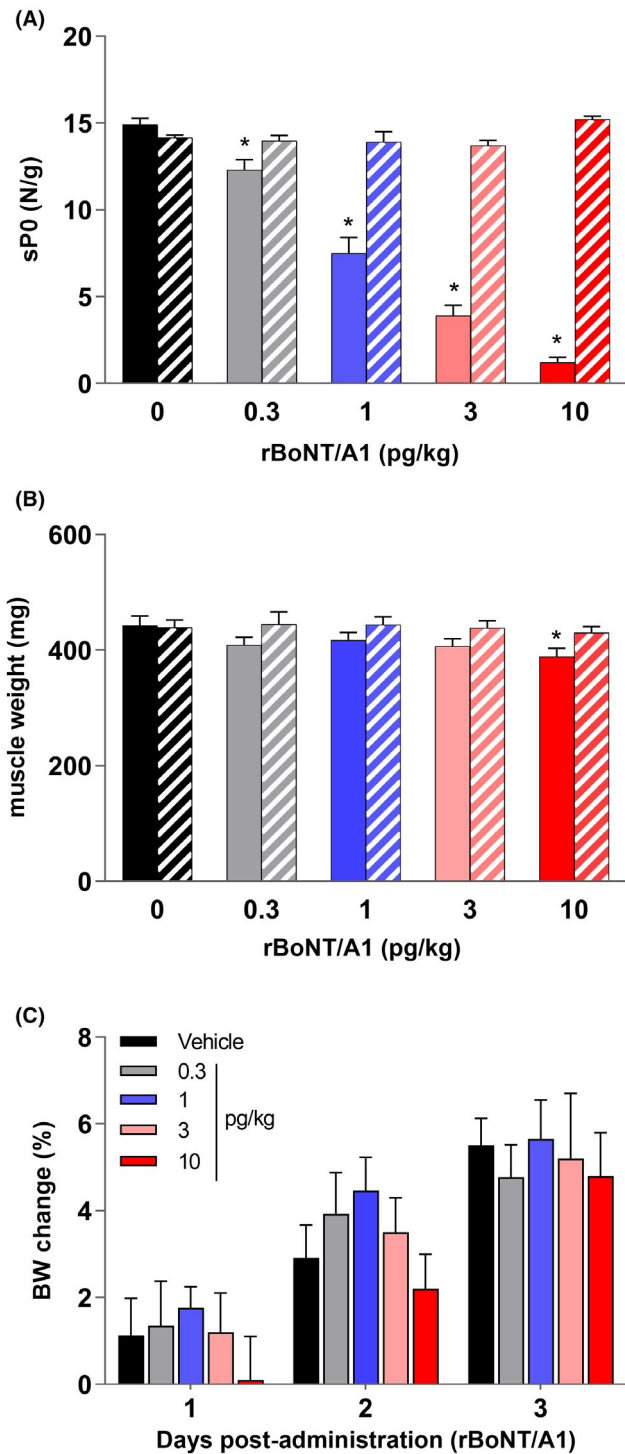


FIGURE 3 (A) The maximal muscle force (N/g) generated by the tibialis anterior (TA) following electrical stimulation of the sciatic nerve, performed 3 days after i.m. injection of rBoNT/A1 (0.3–10 pg/kg) or vehicle (GPB). (B) Weight of the TA muscle (mg) at the end of the experiment. Solid color bars represent the injected (ipsilateral) muscle, whereas striped bars represent the non-injected (contralateral) muscle. (C) Percent change in body weight (vs. day 0) on days 1–3 post-injection of rBoNT/A1 and vehicle (GPB). All values are mean \pm SEM ($n = 6$ /group). * $p < 0.05$ compared with contralateral leg (A and B)

Specifically, muscle weight was reduced by 25% at 5.00 pg/kg, 40%–50% at 25 and 50 pg/kg, and more than 70% at 200 pg/kg compared with the contralateral muscle (Figure 5A). This was accompanied by dose-dependent reductions in muscle volume, up to 30% at 5.00 pg/kg, 40%–55% at 25 and 50 pg/kg, and more than 70% at 200 pg/kg (Figure 5B). No effect of rBoNT/A1 on muscle weight or volume was observed for the contralateral (intact) gastrocnemius lateralis muscle (Figure 5). There was no impact on body weight change in any rBoNT/A1-treated groups (data not shown).

Analysis of the distribution of muscle fibers according to their size showed a pronounced dose-dependent relationship between frequency of distribution and the myofiber area (Figure 6). In rBoNT/A1-injected muscle, there was a dose-dependent increase in the frequency of small fibers (from 0.2 to $1.1 \times 10^3 \mu\text{m}^2$; Figure 6A). For example, there was little or no difference ($\sim 0.03\%$) in distribution frequency of myofiber size of $0.5 \times 10^3 \mu\text{m}^2$ between vehicle-treated and rBoNT/A1-treated group up to 5.00 pg/kg, while the frequency increased to 0.13% with 100 and 200 pg/kg. Conversely, frequencies between each dose were less distinguished in medium to large myofibers (1.2 to $6 \times 10^3 \mu\text{m}^2$), with the 100 and 200 pg/kg groups displaying the most reduced frequency (Figure 6A). The representative images of the muscle cross-section 30 days after injection of vehicle (GPB) or rBoNT/A1 (50 and 200 pg/kg) are presented in Figure 6B.

3.6 | Immunohistochemical analysis of c-SNAP25

The EF14007 specificity for BoNT/A1 cleaved form of SNAP25 was tested in a colocalization experiment with SYSY 111 011, a commercial antibody specific for the full form of SNAP25. SYSY 111 011 can recognize both BoNT/A1 cleaved and non-cleaved forms of SNAP25 because of the localization of its targeted epitope on the SNAP25 protein (N-terminal part; Figure 7A). As shown in Figure 7B, in the injected muscle of vehicle-treated animals, SYSY 111 011 detects SNAP25 protein at NMJ and nerve endings, while there is no labeling observed with EF14007. However, in the muscle of BoNT/A1-treated animals, SYSY 111 011 recognizes SNAP25 N-terminal, whereas EF14007 detects c-SNAP25 resulting in a perfect colocalization as shown in the merged image. These findings confirm EF14007 specificity at detecting only BoNT/A1 cleaved form and not the full form of SNAP25 in the immunohistochemistry assay.

The representative illustrations of c-SNAP25 staining used for scoring is presented in Figure 7C. A single administration of rBoNT/A1 (1.00–200 pg/kg) caused dose-dependent increases in c-SNAP25 staining in NMJs in the injected gastrocnemius lateralis when measured 30 days post-administration (Figure 8). Specifically, there were no or very low levels of staining in muscles injected with either vehicle or 1.00 pg/kg rBoNT/A1. Increased c-SNAP25 staining was observed in muscles injected with 5.00 pg/kg and the scored level of staining reached statistical significance at 25 pg/kg. Maximal c-SNAP25 staining was observed at 50 pg/kg and above (Figure 8).

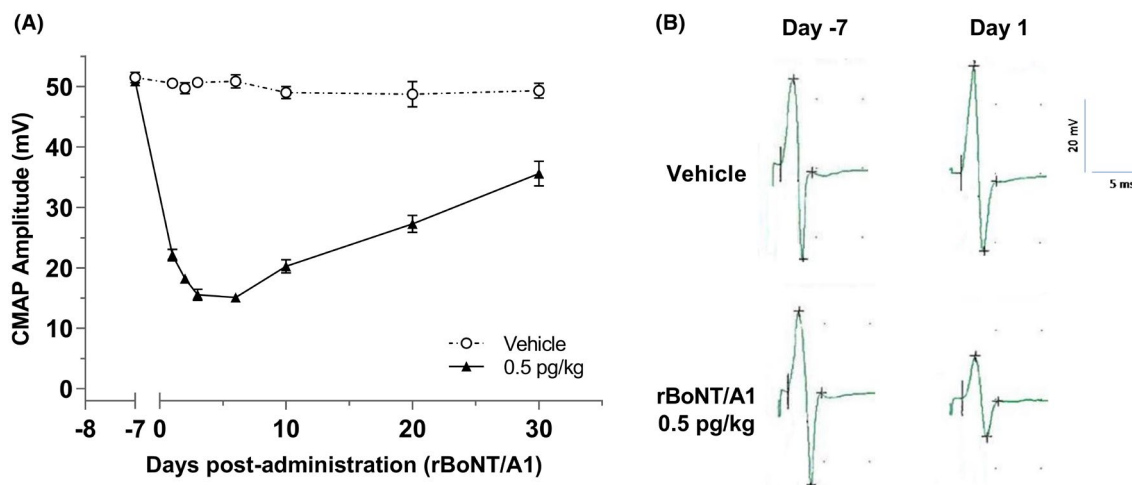


FIGURE 4 (A) The compound muscle action potential (CMAP) amplitude (mV) measured from the lateral gastrocnemius of female Sprague-Dawley rats injected with rBoNT/A1 (0.5 pg/kg) or vehicle (GPB) across days 1–30 postadministration ($n = 8$ –12/group). (B) Representative CMAP recordings at baseline (Day 7) and 24 h (Day 1) after vehicle or rBoNT/A1 0.5 pg/kg administration

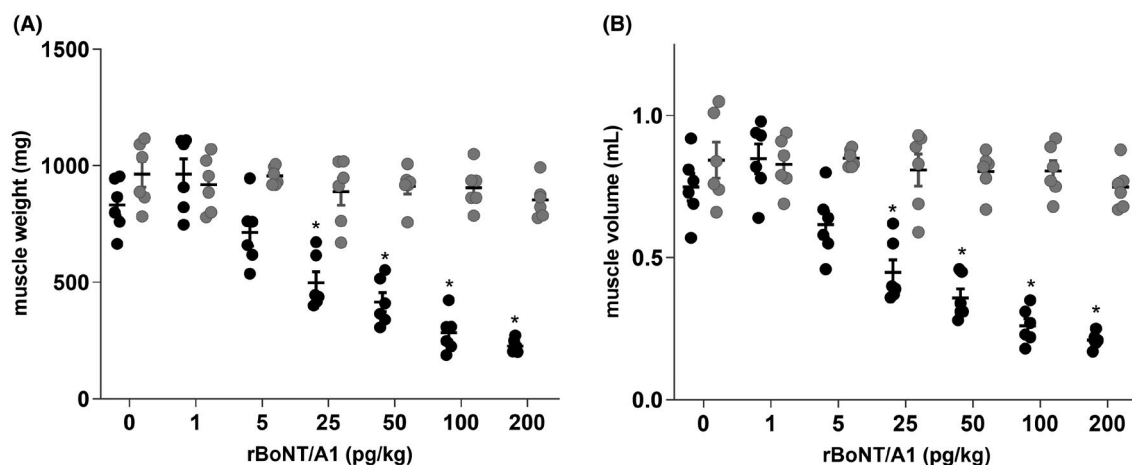


FIGURE 5 Female Sprague-Dawley rats were injected with either rBoNT/A1 (1–200 pg/kg) or vehicle (GPB) into the lateral gastrocnemius, and both ipsilateral (black) and contralateral (gray) muscles were harvested 30 days later for determination of weight (mg; A) and volume (mL; B). * $p < 0.05$ compared with vehicle-injected animals

4 | DISCUSSION

Following on from previous work, in which a novel rBoNT/A1 was synthesized and characterized *in vitro* and *ex vivo*,¹⁵ we evaluated the biologic properties of rBoNT/A1 compared with nBoNT/A1 *in vivo* following acute *i.m.* administration into skeletal muscle.

The DAS assay assesses hind paw muscle weakness after a single BoNT administration into calf muscles. Previously, the efficacy of different BoNT preparations was demonstrated in the DAS assay in mice^{10,27} and in rats.^{4,5,10,28} The DAS assay presents several advantages as it measures (1) the effect of locally administered BoNT on adaptive/functional use of the hind paw (digit abduction), (2) BoNT potency (ED_{50}), (3) kinetics of BoNT, and (4) tolerability. To our knowledge, the present study is the first direct comparison of a recombinant BoNT to its natural analog using the DAS assay. In mice, the potency, onset, time to peak, and duration

of rBoNT/A1 and nBoNT/A1 were comparable. Tolerability profiles were also comparable, as they both resulted in reduced weight gain and weight loss at similar doses. In rats, rBoNT/A1 and nBoNT/A1, injected into the peroneal muscle complex, were comparable in potency, kinetic, and tolerability profiles, confirming similarity of biologic properties.

Mice were less sensitive to rBoNT/A1 and nBoNT/A1 compared with rats when ED_{50} values are converted from pg/animal to pg/kg. For example, the ED_{50} of rBoNT/A1 in mice (48 pg/kg) is over 10-fold higher than in rats (4.3 pg/kg). Interspecies differences in BoNT/A1 sensitivity could be driven, in part, by specific muscle sensitivity, as mice were injected into the gastrocnemius-soleus complex and rats, the peroneal muscle complex. In addition, these complexes are innervated by two separated bifurcations from the sciatic nerve, the tibial nerve for the former, and the common peroneal nerve for the latter. The tibial nerve innervates knee flexors, ankle plantar flexors,

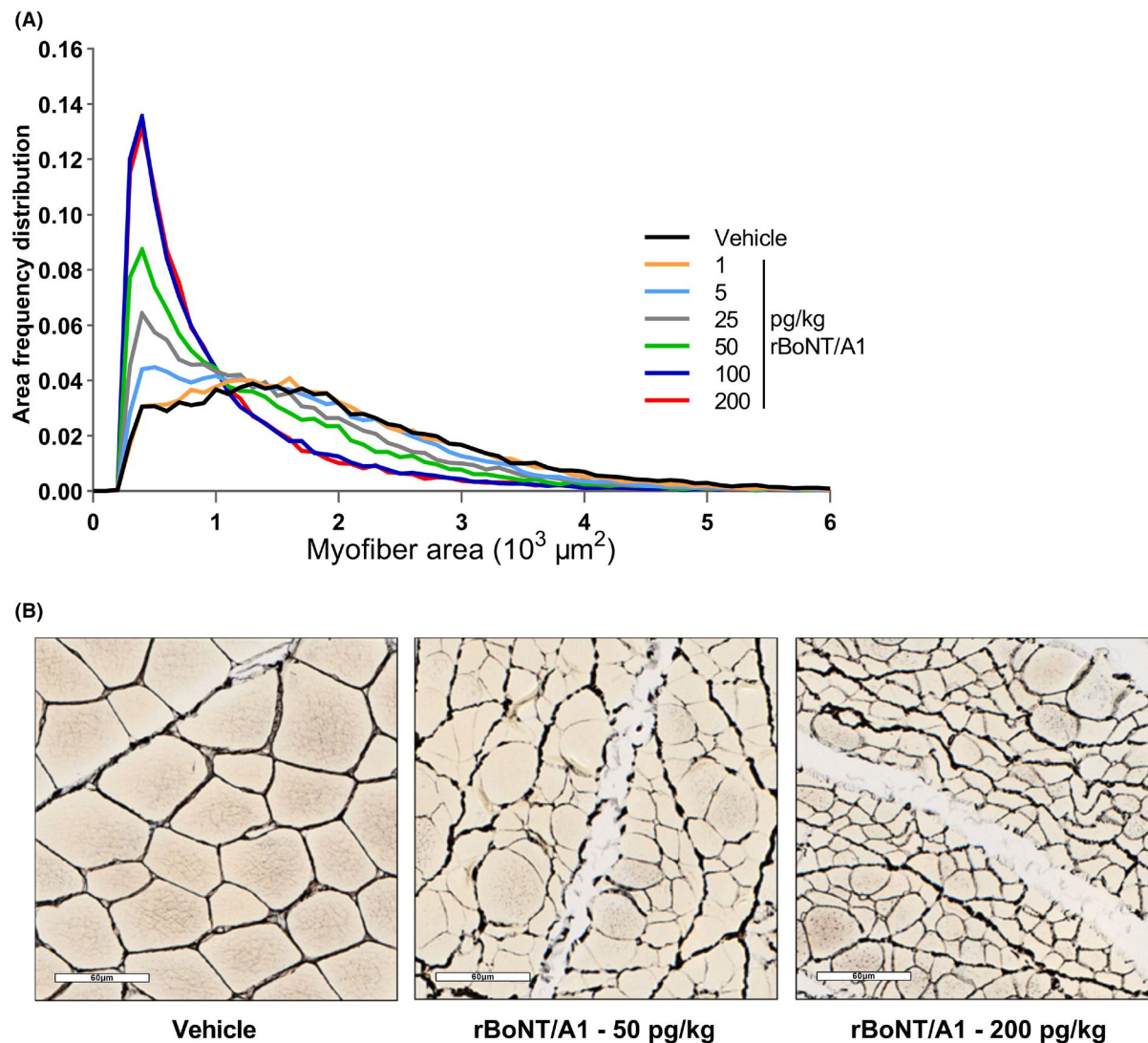


FIGURE 6 The muscle fiber size distribution in the right gastrocnemius lateralis in female Sprague-Dawley rats 30 days after they were injected with rBoNT/A1 (1–200 pg/kg) or vehicle (GPB; $n = 6/\text{group}$; A). The myofiber size distribution was analyzed from a cross-section of the harvested muscle. The area frequency distribution was calculated in intervals of $0.1 \times 10^3 \mu\text{m}^2 \pm \text{SEM}$. (B) The representative images of the muscle cross-section with reticulin staining from female Sprague-Dawley rats injected with vehicle (GPB) or rBoNT/A1 (50 and 200 pg/kg) 30 days earlier (B, scale bar: 60 μm)

and hip motion groups muscles while the common peroneal nerve innervates ankle everters, plantarflexors, and dorsiflexors, including the TA.¹⁹ These muscles are more involved in the digit abduction than the upper muscles. Therefore, as we demonstrated previously in rats, injection into the peroneus muscle complex has a more pronounced effect than in the triceps surae.⁵ Moreover, in rats, the role of muscles adjacent to peroneus, such as the extensor digitorum longus, cannot be excluded as a result of the potential diffusion.⁵ Mice were also less sensitive to onabotulinumtoxinA (onaBoNT/A) compared with rats in a previous DAS assay.⁴ This difference in sensitivity was previously shown to be more pronounced when distinct muscles were injected, gastrocnemius in mice, and tibialis anterior in rats, but less pronounced when the same muscle, gastrocnemius was injected in both species.⁴ Individual muscle versus species differences in sensitivity to BoNT requires further investigation.

As the digit abduction reflex is likely driven by coordinated activity of multiple hindlimb muscles, it is difficult to delineate contribution of a single muscle. To evaluate flaccidity-inducing effects of rBoNT/A1 specific to injected muscle, rBoNT/A1 was tested in the in situ muscle force assay, which has previously been used to evaluate effects of BoNTs on a range of muscles in rodents and in the clinic.^{7,13} rBoNT/A1 caused a dose-dependent reduction in contractile force of the tibialis anterior. Assay sensitivity was higher than that of the DAS, as the potency (ED_{50}) of rBoNT/A1 was markedly higher (1.2 pg/kg) compared with the rat DAS assay (4.3 pg/kg).

We used CMAP to measure direct inhibition of neuromuscular action potential transmission following a single i.m. rBoNT/A1 injection into the gastrocnemius lateralis muscle. CMAP amplitude has a high sensitivity to rBoNT/A1 activity.^{6,31,33} Specifically, inhibition

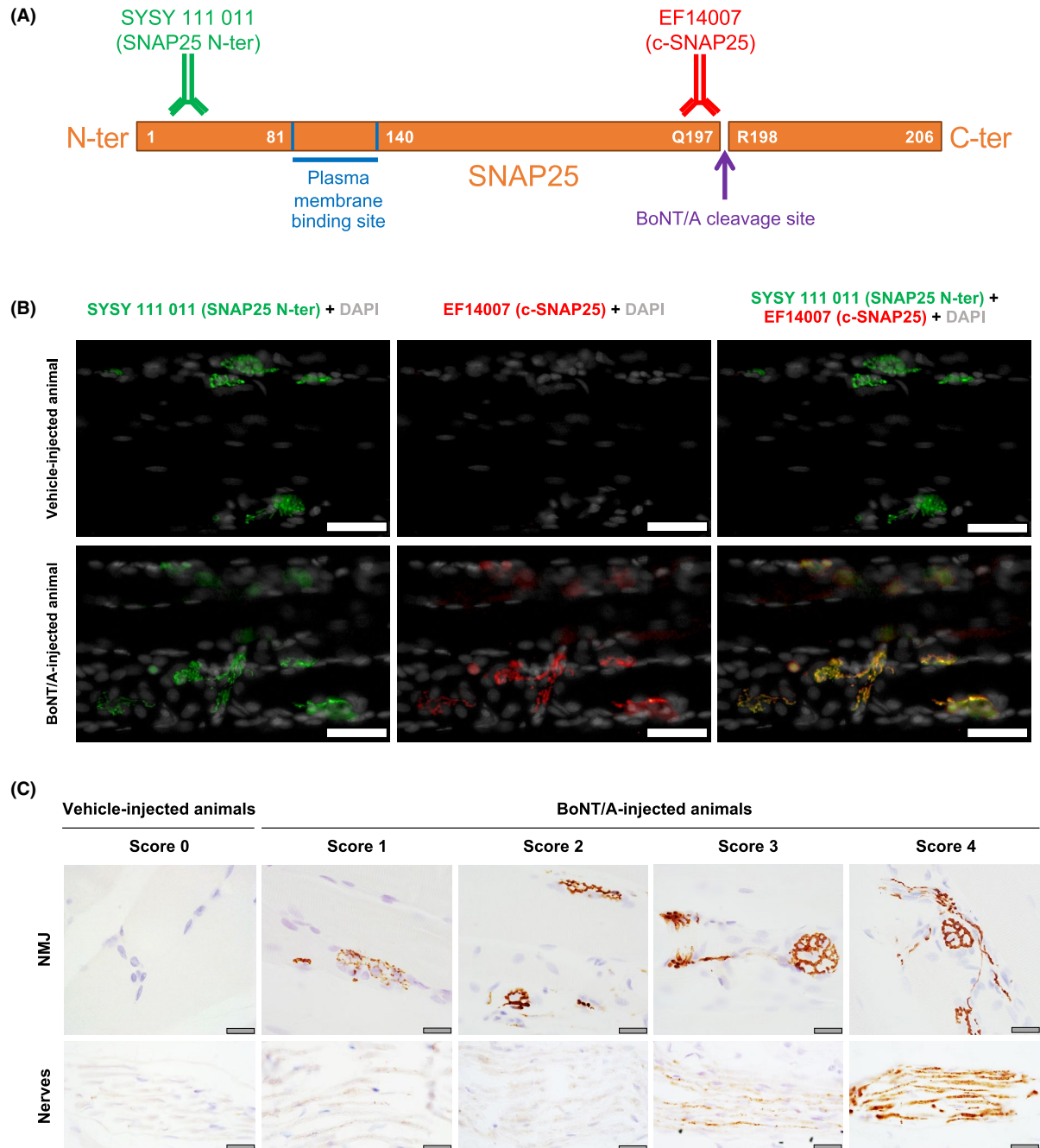


FIGURE 7 (A) Representative images of SNAP25 protein, BoNT/A1 cleavage site and recognition sites for antibodies SYSY 111 011 (N-terminal part) and EF14007 (BoNT/A1 cleavage site). (B) Immunofluorescence colocalization experiment with SYSY 111 011 (green) and EF14007 (red) in injected muscle of vehicle or 200 pg/kg BoNT/A1-treated animals. DAPI (nuclear counterstain) is in light gray. Scale bars: 50 μm . (C) Representative images of c-SNAP25 corresponding to the immunohistochemical scoring system at NMJs, terminal nerve endings, and intramuscular nerves (Nerves) in the gastrocnemius lateralis of female Sprague-Dawley rats following a single i.m. injection of vehicle (GPB) or rBoNT/A1. Illustrations were taken on post-injection days 3–6 (scale bars: 10 μm)

of CMAP amplitude was obtained at a very low rBoNT/A1 dose (0.50 pg/kg) and lasted at least 30 days. Conversely, in the DAS assay, at the dose approaching ED_{50} (4.3 pg/kg), the effect lasted between 8 and 10 days. Thus, functional recovery of the digit abduction reflex can be obtained despite the presence of neuromuscular blockade in at least one muscle involved in the reflex. Full recovery of CMAP amplitude in the injected muscle is then not needed for functional recovery. Alternatively, incomplete functional recovery

(incomplete CMAP amplitude recovery) in the injected muscle remains, but the contribution of other muscles involved in digit abduction reflex compensates for the expression of digit abduction reflex.

We also investigated indirect biologic effects of rBoNT/A1 on muscle mass, volume, and myofibers size following injection into the rat gastrocnemius lateralis. Acute, i.m. injection of 1.00 pg/kg rBoNT/A1 had no effect on morphologic parameters when the muscle was evaluated 30 days after toxin injection. This suggests that

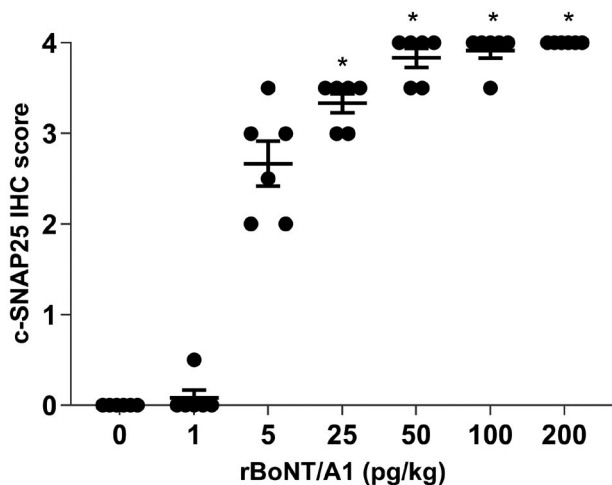


FIGURE 8 Quantification of immunohistochemical labeling of c-SNAP25 in the lateral gastrocnemius muscle taken from female Sprague-Dawley rats 30 days after a single, intramuscular injection of rBoNT/A1 (1–200 pg/kg) or vehicle (GPB; $n = 6/\text{group}$). * $p < 0.05$ compared with vehicle-treated animals

at least 70% inhibition of CMAP amplitude can be obtained without marked changes in muscle morphology at that time point. For higher doses, muscle weight, volume, and myofiber size were similarly affected. From 5.00 pg/kg rBoNT/A1 and above, in line with muscle weight and volume, there was a shift in the myofibers size from large to small, which is consistent with atrophy of the muscle induced by the absence of neural transmission. In accordance with our findings, Na et al.²² observed a similar dose-dependent reduction in muscle weight and volume following a BoNT/A injection into the mouse gastrocnemius-soleus complex. These results were aligned with the in situ muscle force test data, where tibialis anterior muscle weight decreased significantly 3 days post-administration with 10.00 pg/kg of rBoNT/A1 (compared with the non-injected hindlimb), suggesting that muscle atrophy occurred at least from 3 days post-injection. It is also likely that the muscle atrophy occurred in the DAS assay in animals treated with high dose of rBoNT/A1. Nonetheless, muscle mass loss did not fully impair muscle function as animals started to recover to baseline within 4 days of BoNT/A1 administration.

Immunohistochemical detections of c-SNAP25 in rBoNT/A1-treated gastrocnemius lateralis were performed to confirm the enzymatic activity of the novel neurotoxin. Generally, the intensity of c-SNAP25 staining parallels the rBoNT/A1-induced changes in other parameters described above. Interestingly, virtually no c-SNAP25 staining occurred 30 days post-administration of 1.00 pg/kg rBoNT/A1, despite up to 30% decrease in CMAP amplitude. This discrepancy might be linked to limitations in the resolution of c-SNAP25 detection. Nevertheless, these results are consistent with previous findings showing that a low ratio of cleaved/intact SNAP25 correlated well with neural transmission inhibition and muscle flaccidity.^{16,26} Conversely, c-SNAP25 intensity was saturated around 50 pg/kg, while atrophy plateaued around 100 pg/kg or higher, as illustrated by muscle mass decrease. c-SNAP25 is known to form stable non-functional SNARE complexes, which could inhibit neurotransmitter release and

muscle contractility, accentuating muscle atrophy.^{3,17} c-SNAP25 detection 30 days after a single rBoNT/A1 injection at doses as low as 5.00 pg/kg showed good sensitivity of the method to characterize enzymatic activity of the protein within a complex physiologic system.

Recent advances in recombinant technology enable protein engineering to create modified BoNT molecules, characterized with modified biologic properties, such as increased potency, efficacy, duration of action, and improved tolerability. For example, modification of BoNT/B-binding domain results in increased affinity for the human receptor and enhanced properties in vivo.¹² A BoNT/A-derived chimera showed reduced activity at the NMJ but retained activity at nociceptive neurons.²¹ These examples show that recombinant technology is a powerful tool for the development of novel BoNTs with desired clinical properties. Availability of a well-characterized rBoNT/A1, showing comparable activities to nBoNT/A1 with the same amino acid sequence, strengthens confidence in our understanding of structure–function relationships and provides an important source of reference material to support the development of modified recombinant BoNTs.

5 | CONCLUSIONS

Using a range of complementary in vivo assays, we demonstrated that rBoNT/A1 and nBoNT/A1 injected into a skeletal muscle share similar characteristics, including potency, kinetics and tolerability profiles. Additionally, rBoNT/A1 caused a dose-dependent reduction in in situ muscle force and prolonged inhibition of CMAP amplitude, as well as a dose-dependent reduction in weight, volume, and myofiber atrophy of injected skeletal muscle. Furthermore, rBoNT/A1 effects on muscle activity and morphology were accompanied by SNAP25 cleavage in the injected muscle. rBoNT/A1 presents a useful pharmacologic tool that can be used as a reference compound for the characterization of a novel, modified recombinant BoNTs engineered to address unmet clinical needs.

ACKNOWLEDGEMENTS

We would like to thank Denis Carré (Ipsen Innovation) for his precious help on the image acquisition.

DISCLOSURE

Cindy Périer, Vincent Martin, Sylvie Cornet, Christine Favre-Guilhard, Marie-Noelle Rocher, Alban Vignaud, Matthew Beard, Stephane Lezmi, and Mikhail Kalinichev are current or former employees of Ipsen. The research was funded by Ipsen.

DATA AVAILABILITY STATEMENT

Ipsen will share aggregated data that underlie the results reported in this article with qualified researchers who provide a valid research question and subject to an appropriate data-sharing agreement. Study documents, such as the study protocol and study report, are not always available. Proposals should be submitted to DataSharing@Ipsen.com and will be assessed by a scientific review board. Data are available beginning 6 months and ending 5 years after publication; after this time, only raw data may be available.

ORCID

Cindy Périer  <https://orcid.org/0000-0003-4832-9676>

Matthew Beard  <https://orcid.org/0000-0003-3249-7851>

Stephane Lezmi  <https://orcid.org/0000-0002-3412-4058>

Mikhail Kalinichev  <https://orcid.org/0000-0001-6621-6339>

REFERENCES

- Aoki KR. Preclinical update on BOTOX® (Botulinum toxin type a)-purified neurotoxin complex relative to other botulinum neurotoxin preparations. *Eur J Neurol.* 1999;6:S3-S10. doi:10.1111/j.1468-1331.1999.tb00032.x
- Aoki KR. A comparison of the safety margins of botulinum neurotoxin serotypes A, B, and F in mice. *Toxicon.* 2001;39(12):1815-1820. doi:10.1016/S0041-0101(01)00101-5
- Apland JP, Adler M, Oyler GA. Inhibition of neurotransmitter release by peptides that mimic the N-terminal domain of SNAP-25. *J Protein Chem.* 2003;22(2):147-153. doi:10.1023/A:1023423013741
- Broide RS, Rubino J, Nicholson GS, et al. The rat Digit Abduction Score (DAS) assay: a physiological model for assessing botulinum neurotoxin-induced skeletal muscle paralysis. *Toxicon.* 2013;71:18-24. doi:10.1016/j.toxicon.2013.05.004
- Cornet S, Périer C, Kalinichev M. (2020). Optimization of the rat digit abduction score (DAS) assay: evaluation of botulinum neurotoxin activity in the gastrocnemius lateralis, peronei, and extensor digitorum longus. *Toxicon: X*, 6, 100029. doi:10.1016/j.toxcx.2020.100029
- Cornet S, Périer C, Wagner S, Andriambelison E, Pouzet B, Kalinichev M. The use of the dynamic weight bearing test to assess the effects of acute, intramuscularly administered botulinum neurotoxin type A1 in rats. *Toxicon: X*. 2020;7:100041. doi:10.1016/j.toxcx.2020.100041
- Croes SA, Baryshnikova LM, Kaluskar SS, von Bartheld CS. Acute and long-term effects of botulinum neurotoxin on the function and structure of developing extraocular muscles. *Neurobiol Dis.* 2007;25(3):649-664. doi:10.1016/j.nbd.2006.11.007
- Curtis MJ, Alexander S, Cirino G, et al. Experimental design and analysis and their reporting II: updated and simplified guidance for authors and peer reviewers: editorial. *Br J Pharmacol.* 2018;175(7):987-993. doi:10.1111/bph.14153
- Curtis MJ, Bond RA, Spina D, et al. Experimental design and analysis and their reporting: new guidance for publication in BJP: editorial. *Br J Pharmacol.* 2015;172(14):3461-3471. doi:10.1111/bph.12856
- Donald S, Elliott M, Gray B, et al. A comparison of biological activity of commercially available purified native botulinum neurotoxin serotypes A1 to F1 in vitro, ex vivo, and in vivo. *Pharmacol Res Persp.* 2018;6(6):e00446. doi:10.1002/prp2.446
- Durand PD, Couto RA, Isakov R, et al. Botulinum toxin and muscle atrophy: a wanted or unwanted effect. *Aesthetic Surg J.* 2016;36(4):482-487. doi:10.1093/asj/sjv208
- Elliott M, Favre-Guilmond C, Liu SM, et al. Engineered botulinum neurotoxin B with improved binding to human receptors has enhanced efficacy in preclinical models. *Sci Adv.* 2019;5(1):eaau7196. doi:10.1126/sciadv.aau7196
- Frick CG, Richtsfeld M, Sahani ND, Kaneki M, Blobner M, Martyn JAJ. Long-term effects of botulinum toxin on neuromuscular function. *Anesthesiology.* 2007;106(6):1139-1146. doi:10.1097/O1.anes.0000267597.65120.16
- Hackett G, Moore K, Burgin D, et al. Purification and characterization of recombinant botulinum neurotoxin serotype FA, also known as serotype H. *Toxins.* 2018;10(5):195. doi:10.3390/toxins10050195
- Hooker A, Palan S, Beard M. Recombinant botulinum neurotoxin serotype A1 (SXN102342): protein engineering and process development. *Toxins.* 2016;123:S40. doi:10.1016/j.toxicon.2016.11.113
- Jurasinski CV, Lieth E, Dang Do AN, Schengrund C-L. Correlation of cleavage of SNAP-25 with muscle function in a rat model of Botulinum neurotoxin type A induced paralysis. *Toxicon.* 2001;39(9):1309-1315. doi:10.1016/S0041-0101(01)00082-4
- Keller JE, Neale EA. The role of the synaptic protein SNAP-25 in the potency of botulinum neurotoxin type A. *J Biol Chem.* 2001;276(16):13476-13482. doi:10.1074/jbc.M010992200
- Kocaeli H, Yaltirik M, Ayhan M, Aktar F, Atalay B, Yalcin S. Ultrastructural evaluation of intramuscular applied botulinum toxin type A in striated muscles of rats. *Hippokratia.* 2016;20(4):292-298.
- Lorenz MR, Brazill JM, Beeve AT, Shen I, Scheller EL. A neuroskeletal atlas: spatial mapping and contextualization of axon subtypes innervating the long bones of C3H and B6 mice. *J Bone Miner Res.* 2021;36(5):1012-1025. doi:10.1002/jbmr.4273
- Ma J, Elsaidi GA, Smith TL, et al. Time course of recovery of juvenile skeletal muscle after botulinum toxin A injection: an animal model study. *Am J Phys Med Rehabil.* 2004;83(10):774-780. doi:10.1097/O1.PHM.0000137315.17214.93
- Mangione AS, Obara I, Maiarú M, et al. Nonparalytic botulinum molecules for the control of pain. *Pain.* 2016;157(5):1045-1055. doi:10.1097/j.pain.0000000000000478
- Na J, Lee E, Kim Y, et al. Long-term efficacy and safety of a new botulinum toxin type A preparation in mouse gastrocnemius muscle. *Toxicon.* 2020;187:163-170. doi:10.1016/j.toxicon.2020.09.003
- Peck M, Smith T, Anniballi F, et al. Historical perspectives and guidelines for botulinum neurotoxin subtype nomenclature. *Toxins.* 2017;9(1):38. doi:10.3390/toxins9010038
- Pirazzini M, Rossetto O, Eleopra R, Montecucco C. Botulinum neurotoxins: biology, pharmacology, and toxicology. *Pharmacol Rev.* 2017;69(2):200-235. doi:10.1124/pr.116.012658
- Pons L, Vilain C, Volteau M, Picaud P. Safety and pharmacodynamics of a novel recombinant botulinum toxin E (rBoNT-E): Results of a phase 1 study in healthy male subjects compared with abobotulinumtoxinA (Dysport®). *J Neurol Sci.* 2019;407:116516. doi:10.1016/j.jns.2019.116516
- Raciborska DA, Trimble WS, Charlton MP. Presynaptic protein interactions in vivo: evidence from botulinum A, C, D and E action at frog neuromuscular junction: botulinum toxins reveal protein interactions. *Eur J Neurosci.* 1998;10(8):2617-2628. doi:10.1046/j.1460-9568.1998.00270.x
- Roger Aoki K. Botulinum neurotoxin serotypes A and B preparations have different safety margins in preclinical models of muscle weakening efficacy and systemic safety. *Toxicon.* 2002;40(7):923-928. doi:10.1016/S0041-0101(02)00086-7
- Rosales RL, Bigalke H, Dressler D. Pharmacology of botulinum toxin: differences between type A preparations. *Eur J Neurol.* 2006;13:2-10. doi:10.1111/j.1468-1331.2006.01438.x
- Rossetto O, Pirazzini M, Montecucco C. Botulinum neurotoxins: genetic, structural and mechanistic insights. *Nat Rev Microbiol.* 2014;12(8):535-549. doi:10.1038/nrmicro3295
- Rudkin B, Cluet D & Spichy M Method for identifying cells in a biological tissue. (European Patent No EP2901415 (B1)).
- Sakamoto T, Torii Y, Takahashi M, et al. Quantitative determination of the biological activity of botulinum toxin type A by measuring the compound muscle action potential (CMAP) in rats. *Toxicon.* 2009;54(6):857-861. doi:10.1016/j.toxicon.2009.06.020
- Steward L, Brin MF, Brideau-Andersen A. Novel native and engineered botulinum neurotoxins. *Handb Exp Pharmacol.* 2021;263:63-89. doi:10.1007/164_2020_351
- Torii Y, Goto Y, Takahashi M, et al. Quantitative determination of biological activity of botulinum toxins utilizing compound muscle action potentials (CMAP), and comparison of neuromuscular transmission blockage and muscle flaccidity among toxins. *Toxicon.* 2010;55(2-3):407-414. doi:10.1016/j.toxicon.2009.09.005

34. Tsai F-C, Hsieh M-S, Chou C-M. Comparison between neurectomy and botulinum toxin A injection for denervated skeletal muscle. *J Neurotrauma*. 2010;27(8):1509-1516. doi:10.1089/neu.2010.1320
35. Ward SR, Minamoto VB, Suzuki KP, Hulst JB, Bremner SN, Lieber RL. Recovery of rat muscle size but not function more than 1 year after a single botulinum toxin injection: persistent changes in muscle after BT-A. *Muscle Nerve*. 2018;57(3):435-441. doi:10.1002/mus.25707
36. Webb RP. Engineering of botulinum neurotoxins for biomedical applications. *Toxins*. 2018;10(6):231. doi:10.3390/toxins10060231
37. Weisemann J, Krez N, Fiebig U, et al. Generation and characterization of six recombinant botulinum neurotoxins as reference material to

serve in an international proficiency test. *Toxins*. 2015;7(12):5035-5054. doi:10.3390/toxins7124861

How to cite this article: Périer C, Martin V, Cornet S, et al. Recombinant botulinum neurotoxin serotype A1 in vivo characterization. *Pharmacol Res Perspect*. 2021;9:e00857. <https://doi.org/10.1002/prp2.857>